Differences in Membrane Fluidity and Fatty Acid Composition between Phenotypic Variants of *Streptococcus pneumoniae*

Barak Aricha,[1] Itzhak Fishov,[2] Zvi Cohen,[3] Noga Sikron,[1] Stella Pesakhov,[1]
Inna Khozin-Goldberg,[3] Ron Dagan,[1] and Nurith Porat[1]*

*Pediatric Infectious Disease Unit, Soroka University Medical Center, Faculty of Health Sciences,[1] Microalgal
Biotechnology Laboratory, A. Katz Department of Dry Lands Biotechnologies, J. Blaustein Institute for
Desert Research, Sde Boker Campus,[3] and Department of Life Sciences,
Ben-Gurion University of the Negev,[2] Beer Sheva, Israel*

Phase variation in the colonial opacity of *Streptococcus pneumoniae* has been implicated as a factor in the pathogenesis of pneumococcal disease. This study examined the relationship between membrane characteristics and colony morphology in a few selected opaque-transparent couples of *S. pneumoniae* strains carrying different capsular types. Membrane fluidity was determined on the basis of intermolecular excimerization of pyrene and fluorescence polarization of 1,6-diphenyl 1,3,5-hexatriene (DPH). A significant decrease, 16 to 26% ($P \leq 0.05$), in the excimerization rate constant of the opaque variants compared with that of the transparent variants was observed, indicating higher microviscosity of the membrane of bacterial cells in the opaque variants. Liposomes prepared from phospholipids of the opaque phenotype showed an even greater decrease, 27 to 38% ($P \leq 0.05$), in the pyrene excimerization rate constant compared with that of liposomes prepared from phospholipids of bacteria with the transparent phenotype. These findings agree with the results obtained with DPH fluorescence anisotropy, which showed a 9 to 21% increase ($P \leq 0.001$) in the opaque variants compared with the transparent variants. Membrane fatty acid composition, determined by gas chromatography, revealed that the two variants carry the same types of fatty acids but in different proportions. The trend of modification points to the presence of a lower degree of unsaturated fatty acids in the opaque variants compared with their transparent counterparts. The data presented here show a distinct correlation between phase variation and membrane fluidity in *S. pneumoniae*. The changes in membrane fluidity most probably stem from the observed differences in fatty acid composition.

Phase variation in the colonial opacity of *Streptococcus pneumoniae* has been implicated as a factor in the pathogenesis of pneumococcal disease (27). The different appearance of bacterial colonies is assumed to result from the spontaneous and reversible phase variation of surface components, the identity of which is not yet clear. The frequency of switching is highly variable from isolate to isolate, ranging from 10^{-3} to 10^{-6} per generation. The significance of opacity variation in the biology of pneumococcal infection in vivo was examined by using animal models of nasopharyngeal colonization and bacteremia. Transparent variants persist in the nasopharynx in vivo and show greater adherence to human lung epithelial cells. However, experiments performed with an adult mouse model of sepsis showed a strong selection for organisms with the opaque morphology during invasive infections (28).

Genetic experiments were used to isolate a single locus able to confer altered colony opacity at a higher frequency than the background rate (18). The opacity locus was found to be associated with two genes in the presumed glycerol operon, *glpF* and *glpD*, required for glycerol metabolism in other bacteria. This finding raises the possibility that phase variation in *S. pneumoniae* is linked to the mechanism of synthesis of membrane phospholipids where glycerol is one of the major building blocks.

The linkage between membrane characteristics and cell physiology has been widely covered in the literature (17, 20). Many processes associated with cell growth and cell function are accompanied by changes in membrane characteristics. One example is the phenomenon of "homeoviscous adaptation" in membranes of bacteria, where changes in growth temperature or hydrostatic pressure induce changes in the activities of enzymes involved in fatty acid metabolism by altering the proportion of unsaturated fatty acids in their phospholipids (8, 26).

In this report we examine the hypothesis that pneumococci use an analogous adaptation machinery involving changes in their cytoplasmic membrane. The present work demonstrates a linkage between phase variation in colony morphology and the biophysical and biochemical characteristics of the membrane bilayer in selected opaque and transparent variants of *S. pneumoniae*.

MATERIALS AND METHODS

Bacterial strains and growth conditions. Four opaque-transparent variants of *S. pneumoniae* were included in this study (kindly provided by J. N. Weiser, University of Pennsylvania); the two variants of each strain were isolated from the same ancestor colony (Table 1). The capsular type was confirmed by the quellung reaction (4) with antisera provided by the Statens Serum Institute of Copenhagen, Denmark. The identity in the genetic background of each pair was confirmed by pulsed-field gel electrophoresis (21) (Fig. 1). All strains were cultured in brain heart infusion (BHI) broth (Difco Laboratories, Becton, Dick-

* Corresponding author. Mailing address: Pediatric Infectious Disease Unit, Soroka University Medical Center, P.O. Box 151, Beer Sheva 84101, Israel. Phone: 972-8-6400839. Fax: 972-8-6232334. E-mail: npurat@bgumail.bgu.ac.il.

TABLE 1. Pneumococcal strains used in this study

Strain	Type	Relevant characteristic	Reference
P71	18C	Opaque variant of clinical isolate p68	11
P73	18C	Transparent variant of clinical isolate p68	11
P376	6A	Opaque variant of clinical isolate p303	11
P384	6A	Transparent variant of clinical isolate p303	11
P382	6B	Opaque variant of clinical isolate p324	11
P383	6B	Transparent variant of clinical isolate p324	11
23F Op	23F	Opaque variant of clinical isolate Rnp6	This study
23F Tr	23F	Transparent variant of clinical isolate Rnp6	This study

inson and Company, Sparks, Md.) supplemented with 5% horse serum (Biological Industries, Beit Haemek, Israel). The strains were grown at 37°C with aeration until they reached an optical density at 620 nm (OD_{620}) of 0.2. Broth cultures were plated onto tryptic soy plates with 1% agar (Hy-Labs, Rehovot, Israel), onto which 5,000 U of catalase (Worthington Biochemical, Freehold, N.J.) was spread, and incubated at 37°C in a candle extinction jar (27). Colony morphology was determined under magnification and oblique transmitted illumination as described by Weiser et al. (27).
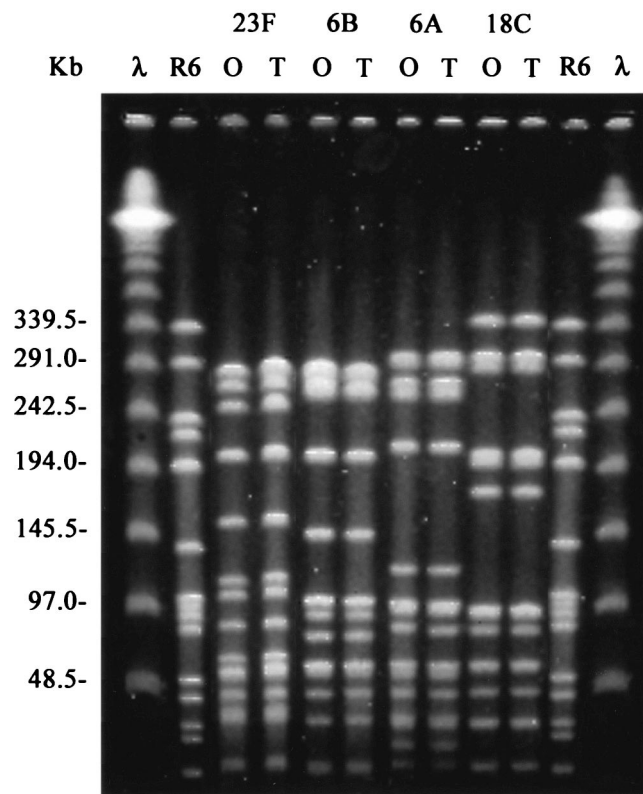

FIG. 1. Pulsed-field gel electrophoresis patterns generated by SmaI digestion of opaque (O) and transparent (T) variants of *S. pneumoniae* strains belonging to serotypes 23F, 6B, 6A, and 18C. λ, lambda ladder; R6, *S. pneumoniae* reference strain used as a molecular weight marker.

Measurements of membrane lateral diffusion. Lateral diffusion of the fatty acyl chains was measured by the intermolecular excimerization of pyrene. This fluorescent probe, when excited by light, can form a complex with an identical unexcited probe molecule. Such a complex is called an excimer and is recognized by the production of a new fluorescent band at a longer wavelength than the usual emission spectrum of the monomer. The rate of excimer formation depends on three parameters: pyrene concentration (C_{Py}), excimer lifetime (τ_{Py}), and the diffusion rate constant (k_a). The excimer-to-monomer ratio increases linearly with the pyrene concentration. The probe's lateral diffusion can be derived from the slope of the curve as follows: excimer/monomer = $k_a\tau_{Py}C_{Py}$ (9).

Samples of bacterial cultures at steady-state growth, $OD_{450} = 0.25$, were fixed by formaldehyde (final concentration, 0.25%), washed twice with phosphate-buffered saline (PBS) containing 0.25% formaldehyde (pH 7.4), and incubated with increasing concentrations of pyrene, 0.1 to 0.4 μM (added as a 10^{-4} M solution in ethanol). The extent of incorporation of the probe was not significantly different for any of the strains used. An unlabeled portion of the sample, incubated under the same conditions, served as a scattering reference (less than 1% of the intensity of the labeled sample). Measurements were carried out at 37°C with a benchtop continuous spectrofluorometer (Ratio Master; Photon Technology International, Inc.) with excitation at 335 nm, emission at 373 nm (for the monomer) and 470 nm (for the excimer), and 4- and 4-nm slits, respectively (25).

Measurement of fluorescence anisotropy. Measurement of fluorescence anisotropy is used for studying the rotational diffusion of the fatty acyl chains in the membrane interior. The sample is excited with polarized light, and the emitted light is polarized to a different extent, depending on, among other factors, the angle between the absorption and emission dipole moments of the probe and its rotational Brownian motion during the excited-state lifetime. The magnitude of the rotational Brownian motion depends on the size and shape of the probe molecule and its surrounding microviscosity and temperature.

Fluorescence anisotropy is defined as the ratio of polarized components to the total intensity by the equation A = $I_{II} - I_\perp/I_{II} + 2I_\perp$, where I_{II} and $I_\perp$ are the fluorescence intensities parallel and perpendicular to the direction of the excitation light beam. Anisotropy of DPH (1,6-diphenyl 1,3,5-hexatriene) was used to monitor changes in membrane dynamics, as described previously (29). Briefly, samples of bacterial cultures at steady-state growth, $OD_{450} = 0.25$, were fixed by formaldehyde (final concentration, 0.25%), washed twice with PBS containing 0.25% formaldehyde (pH 7.4), and then incubated for 1 h at 37°C with 5×10^{-6} M DPH (added as a 10^{-4} M solution in tetrahydrofuran). Unlabeled organisms served as a scattering reference (less than 3% of the intensity of the labeled sample). Steady-state fluorescence anisotropy was measured at 37°C with a Perkin-Elmer LS50B spectrofluorometer (Perkin-Elmer Ltd., Beaconsfield, England) with excitation at 360 nm and emission at 430 nm, 2.5- and 2.5-nm slits, respectively, and a 3-s integration time.

Lifetime measurements. Changes in pyrene excimerization rate constants and DPH anisotropy are interpreted here in terms of variation in viscosity after verifying that the DPH and pyrene lifetimes are constant under the conditions studied. DPH and pyrene lifetime measurements of were carried out with a single-photon counting spectrofluorometer (FLS 920; Edinburgh Instruments) under the conditions studied.

Preparation of liposomes. Bacterial phospholipids were extracted by the methanol-chloroform method under nonoxidizing conditions and dried (3). Dry phospholipids were resuspended in PBS, and liposomes were prepared by gentle sonication (model VCX 750; Sonics and Materials Inc., Newtown, Conn.) three times for 30 s each time at 200 W. To determine phospholipid concentrations, phosphorus content was determined by the method of Lanzetta et al. (12). The pyrene excimerization rate constant was determined in solutions containing 0.5 mM phospholipids. The extent of incorporation of the probe was not significantly different for any of the liposome types.

Fatty acid extraction and analysis. Lipids were extracted from lyophilized biomass with chloroform and methanol as described by Bligh and Dyer (6) and separated by two-dimensional thin-layer chromatography. Lipids were transmethylated with 2% H_2SO_4 in methanol at 70°C for 1 h (7). The resulting fatty acid methyl esters were analyzed by gas chromatography on a Supelcowax 10 with a temperature gradient of 185 to 225°C as previously described (7). A known amount of an internal standard ($C_{17:0}$) was added to each sample to allow for lipid quantitation. Fatty acid methyl esters were identified by cochromatography with authentic standards (Sigma Chemical Co.) and by comparison of their equivalent chain lengths (1).

Statistical analysis. The significance of differences between opaque and transparent variants was determined by the unpaired *t* test.
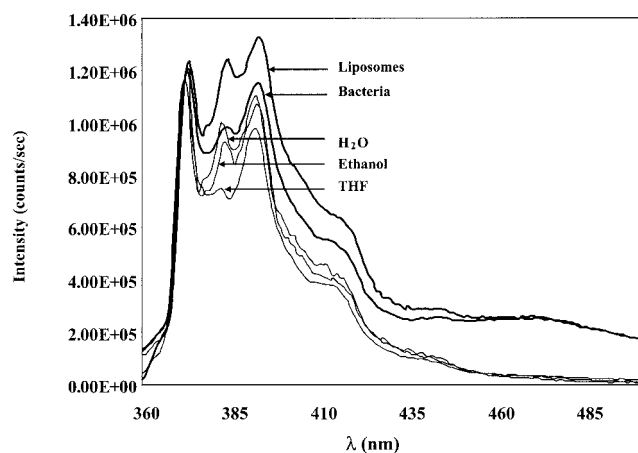
FIG. 2. Fluorescence emission spectra of 0.2 μM pyrene (excitation at 335 nm), normalized by the intensity of the first emission band at 373 nm, in three different solvents (water, ethanol, and tetrahydrofuran [THF]), in bacteria, and in liposomes.

RESULTS

Membrane dynamic characteristics in whole bacteria and their relation to phase variation. (i) Monitoring by pyrene excimerization. Two observations confirm that the probe was inserted into the membrane. First, the emission spectrum of pyrene in dilute solutions depends on solvent polarity (22). The ratio of the fluorescence intensities of the first ($\lambda = 373$ nm), third ($\lambda = 383$ nm), and fourth ($\lambda = 395$ nm) vibronic bands of the pyrene emission spectra was used to sense the polarity of the environment where the probe molecule is inserted. Figure 2 shows the emission spectra of pyrene (normalized by the intensity of the first emission band at 373 nm) in different solvents (water, ethanol, and tetrahydrofuran), as well as in bacteria and in liposomes. The overall shape of the pyrene emission spectra in bacteria and in liposomes presented was typical of all four of the strains included in this study. The low concentrations of pyrene used in our experiments dictated wider slits in order to get a reasonable fluorescence intensity. Therefore we had to use 4-nm slits, which provided an adequate compromise between resolution and sensitivity. The three resolved vibronic bands were successfully used to sense the polarity of the probe's environment. While the shift in the location of the emission maxima is small, the ratio of the three major emission bands of the monomer (bands I, III, and IV) changes considerably with solvent polarity. Table 2 shows the ratio of the three major emission bands of pyrene monomer.

TABLE 2. Ratios of the three major pyrene monomer emission bands in different solvents, in bacteria, and in liposomes

Solvent	Dielectric constant	$I_{373}{:}I_{383}{:}I_{395}$[a] ratio	I_{373}/I_{395} ratio	I_{373}/I_{383} ratio
Liposomes	ND[b]	1:1.06:1.14	0.88	0.94
Bacteria	ND	1:0.84:0.98	1.11	1.19
Tetrahydrofuran	2.95	1:0.79:0.92	1.08	1.26
Ethanol	24.3	1:0.86:0.95	1.05	1.16
Water	81	1:0.63:0.84	1.19	1.60

[a] The intensity of the first emission band at 373 nm (I_{373}) was normalized to 1, and the two other emission bands were calculated accordingly.
[b] ND, not determined.

The intensity of the emission bands at 383 and 395 nm is higher in less polar solvents than in polar solvents. The vibronic profile of pyrene in bacteria and liposomes resembles that of pyrene in less polar solvents, suggesting that the probe was inserted into the hydrophobic lipid bilayer. Second, the total concentration of pyrene in the suspension of the labeled cells is 0.2 μM, which is too low for noticeable formation of excimers in a homogeneous solution (25). The appearance of the excimer peak (at 470 nm) in the fluorescence spectra of bacterial cells and liposomes (Fig. 2) is thus indicative of a much higher local concentration of the probe partitioned into the membrane.

Membrane microviscosity in four opaque-transparent pairs, each pair carrying a different capsular type, was examined by measuring the lateral diffusion of pyrene (Table 3). A significant decrease in the pyrene excimerization rate constant, 16 to 26% ($P \leq 0.05$), was measured in the opaque variants compared with the transparent variants. Pyrene excimer lifetime measurements were also carried out in order to show that the decrease in the pyrene excimerization rate constant in the opaque variants compared with that in the transparent variants was due to reduced lateral diffusion of the probe molecules rather than to a shorter excimer fluorescence lifetime, according to the equation excimer/monomer = $k_a \tau_{Py} C_{Py}$. The conserved pyrene lifetime in each of the two opaque-transparent variants (Table 3) verifies that the decrease in the excimerization rate constants in the opaque variants is due, at least in part, to a lower rate of lateral diffusion of the probe, indicating increased membrane microviscosity in the opaque variant.

(ii) Monitoring by DPH anisotropy. Membrane microviscosity was also estimated by measuring the rotational diffusion of the fatty acyl chains in the membrane interior. This was done by the method of steady-state fluorescence anisotropy with DPH as a probe (Table 4). The results show a 9 to 21%

TABLE 3. Pyrene excimerization rate constants in four opaque-transparent pairs of *S. pneumoniae*[a]

Serotype	Excimerization rate constant (K)		% Difference[b]	Lifetime (ns)	
	Transparent	Opaque		Transparent	Opaque
6A	0.592 ± 0.040	0.474 ± 0.034	25	59.88	59.74
6B	0.475 ± 0.027	0.377 ± 0.018	26	63.53	64.78
18C	0.498 ± 0.075	0.404 ± 0.008	23	55.81	56.30
23F	0.302 ± 0.033	0.261 ± 0.026	16	53.31	58.69

[a] Values represent the mean of at least five determinations in triplicate plus the standard deviation. $P \leq 0.05$ for the difference between excimerization rate constants in opaque and transparent variants.
[b] Calculated by the formula $(K_{Tr} - K_{Op})/K_{Op} \times 100$.

TABLE 4. DPH anisotropy in three opaque-transparent pairs of *S. pneumoniae*[a]

Serotype	Anisotropy (A)		% Difference[b]	Lifetime (ns)	
	Transparent	Opaque		Transparent	Opaque
6A	0.178 ± 0.002	0.201 ± 0.007	13	9.29	9.26
6B	0.180 ± 0.007	0.196 ± 0.005	9	9.41	9.48
18C	0.151 ± 0.001	0.182 ± 0.003	21	9.42	9.33

[a] Values represent the mean of at least three determinations in triplicate plus the standard deviation. $P \leq 0.001$ for the difference in anisotropy between opaque and transparent variants.
[b] Calculated by the formula $(A_{Op} - A_{Tr})/A_{Tr} \times 100$.

increase in the anisotropy value ($P \leq 0.001$) in the opaque variants compared with the transparent variants, indicating increased microviscosity of the lipid core associated with the opaque phenotype. DPH lifetimes measured by single-photon correlation were practically identical for each opaque-transparent pair, suggesting that the different anisotropy values between the opaque and transparent variants result from changes in membrane viscosity.

Membrane dynamic characteristics in liposomes. To verify that the difference in membrane fluidity originates from the lipids, pyrene excimerization was examined in liposomes, which were reconstructed from purified lipids of the opaque and transparent phenotypes. As summarized in Table 5, liposomes reconstructed from phospholipids of the opaque variant showed a significant decrease in the pyrene excimerization rate constant compared to liposomes that were created from phospholipids of the transparent variant, 27 to 38% ($P \leq 0.05$). Pyrene lifetimes in liposomes were very similar for each opaque-transparent pair (Table 5). The difference between the opaque and transparent variants of each pair was even more prominent when measured in liposomes compared to the results in whole bacteria (Table 3), suggesting that the increased membrane microviscosity in the opaque variants is due, at least in part, to differences in their lipid compositions.

Fatty acid analysis. Gas chromatographic analysis of fatty acid methyl ester composition was performed on four opaque-transparent pairs. In Table 6, the relative percentages of the cell fatty acids of two *S. pneumoniae* opaque-transparent pairs are reported. The two variants carry the same types of fatty acyl residues, mainly saturated and unsaturated straight C_{16} and C_{18} acids. However, the proportions of the various fatty acids varied. For each serotype and phase variant we have calculated the desaturation index as the weighted average of the number of double bonds per fatty acid. The most noticeable difference between the two variants was the degree of unsaturation, which was higher in the transparent variants than in the opaque variants. For serotype 6A, the desaturation index was 0.41 in the transparent variant and 0.32 in the opaque variant (28% difference); for serotype 6B, it was 0.51 in the transparent variant and 0.40 in the opaque variant (28% difference); for serotype 18C, it was 0.41 in the transparent variant and 0.31 in the opaque variant (32% difference); and for serotype 23F, it was 0.46 in the transparent variant and 0.38 in the opaque variant (21% difference).

DISCUSSION

Variability and adaptability are crucial characteristics of organisms possessing the ability to survive and prosper under various environmental conditions (2). *S. pneumoniae* has the ability to thrive in a number of different host environments, including the bloodstream and the mucosal surfaces of the upper respiratory tract. The pneumococcus, when grown under different conditions, undergoes spontaneous and reversible phase variation, which is apparent as differences in colony opacity on transparent agar surfaces. Phase variation involves changes in the amount of phosphorylcholine and the amounts of several important surface proteins (28). The nature of the mechanism controlling phase variation is still under investigation.

A universal conserved adaptation response observed among bacteria is adjustment of the membrane lipid composition to various growth conditions. It has been shown (10) that the general response mechanism of certain thermotolerant strains or species to superoptimal temperatures, as well as to oxidative stress, is associated with an increased degree of fatty acid unsaturation or decreased fatty acid chain length. The changes in lipid composition enable the microorganisms to maintain

TABLE 5. Pyrene excimerization rate constant in liposomes that were reconstructed from purified phospholipids of the opaque and transparent phenotypes[a]

Serotype	Excimerization rate constant (K)		% Difference[b]	Lifetime (ns)	
	Transparent	Opaque		Transparent	Opaque
6A	0.481 ± 0.003	0.349 ± 0.049	38	73.3	63.9
6B	0.409 ± 0.028	0.322 ± 0.027	27	75.8	78.0
18C	0.328 ± 0.014	0.227 ± 0.022	31	80.8	77.6
23F	0.372 ± 0.038	0.231 ± 0.034	38	83.1	84.4

[a] For 6A, 18C, and 23F, opaque and transparent values represent the mean of at least five determinations plus the standard deviation; for 6B, the values represent the mean of two determinations plus the standard deviation. $P \leq 0.05$ for the difference between excimerization rate constants in opaque and transparent variants.
[b] Calculated by the formula $(K_{Tr} - K_{Op})/K_{Op} \times 100$.

TABLE 6. Fatty acid compositions of opaque and transparent phase variants of *S. pneumoniae*[a]

Serotype	Fatty acid composition (% of total fatty acids)													UI[b]
	12:0	14:0	14:1	16:0	16:1 Δ7	16:1 Δ9	16:1 Δ11	18:0	18:1 Δ9	18:1 Δ11	18:1[c]	18:2	20:1	
6A Op	5.6	9.4	1.6	44.2	1.5	10.6	0.9	8.9	3.1	10.0	0.3	1.7	0.2	0.32
6A Tr	4.8	8.3	1.9	39.0	2.8	15.8	1.6	6.5	2.2	14.7	0.6	0.5	0.5	0.41
6B Op	5.0	13.7	1.3	38.5	3.4	15.5	1.8	2.4	2.3	14.0	0.5	0.5	0.5	0.40
6B Tr	1.8	6.2	0.7	35.8	3.4	12.9	1.9	4.6	4.2	25.1	0.8	0.8	0.8	0.51
18C Op	10.9	11.8	2.7	41.4	1.9	14.3	1.0	4.3	1.4	8.8	0.0	0.5	0.0	0.31
18C Tr	6.4	8.8	2.4	37.4	2.4	14.4	1.5	5.4	2.2	17.0	0.5	0.2	0.0	0.41
23F Op	5.4	9.8	1.4	42.4	2.8	13.8	1.3	4.6	2.7	12.5	0.4	1.0	0.4	0.38
23F Tr	4.1	7.7	1.7	37.8	3.1	15.1	1.8	4.6	2.8	17.3	0.8	0.9	0.4	0.46

[a] Op, opaque; Tr, transparent. For serotype 6A (Op and Tr), values are the means of triplicate determinations of seven independent experiments; for 6B and 18C (Op and Tr), values are the means of triplicate determinations of two independent experiments; and for 23F (Op and Tr), values are the means of triplicate determinations of three independent experiments.

[b] UI, unsaturation index, defined as the weighted average of the number of double bonds per fatty acid.

[c] Unidentified isomer.

membrane biophysical characteristics and biochemical functions in the face of environmental fluctuations.

The cell membrane of the pneumococcus is a typical bilayer composed mainly of various phospholipids, glycolipids, and proteins (23). Changes in lipid composition, like the degree of unsaturation of fatty acyl chains and their length and degree of branching, result in alterations in the biophysical characteristics of the membrane. The dynamic characteristics are expressed by the so-called "membrane microviscosity" parameter, which relates to the physical state of the lipid acyl chains. One can describe three distinctive modes of motion of the acyl chains as (i) lateral diffusion of individual molecules within the face of the bilayer, (ii) rotational diffusion of the fatty acyl chains in the bilayer interior, and (iii) transbilayer diffusion ("flip flop"), which is quite rare. In the course of the present study, membrane characteristics were documented in phase variants of *S. pneumoniae*. We used two different fluorescence assay methods that provide information on the two diffusion modes.

To avoid any changes caused by enzymatic activities during labeling and measurements, formaldehyde fixation was used during sample preparation. As reported before (5) and checked by us for each strain used in this study, fixation itself had no effect on either pyrene lateral diffusion or the fluorescence anisotropy of DPH (data not shown).

The rate of lateral diffusion of membrane phospholipids was evaluated by determining the intermolecular excimerization of pyrene. The monomer of this highly hydrophobic molecule exhibits five well-resolved major vibronic bands between 370 and 400 nm generally labeled I to V in progressive order. The ratio of the emission intensities of vibronic bands I, III, and IV depends on solvent polarity and is therefore commonly used to characterize the polarity of structured and unisotropic media like micelles and biological membranes (22). Although the probe molecules may be distributed in the membrane at different sites and depths, having a distinct type of polarity, the spectra represent an average of the emission characteristics of the environment sensed by the individual probe molecules. The emission spectra of pyrene and the intensity ratios (listed in Table 2) in bacteria and in liposomes clearly show that pyrene was immersed in a nonpolar environment, namely, the membrane.

Differences in the lateral diffusion of pyrene were found for the two colony morphologies when measured in four opaque-transparent pairs of different serotypes. The excimerization rate constants in the opaque variants were significantly lower than those in their transparent counterparts (16 to 26%, $P \leq 0.05$), indicating higher membrane microviscosity in the opaque variants than in the transparent variants. The pyrene lifetime, measured under the conditions studied, showed no change, thus supporting our interpretation that the difference in the pyrene excimerization rate constants was linked to variation in membrane microviscosity.

It is well known that polypeptides, proteins, and other non-lipid membrane constituents may significantly reduce the lateral diffusion of lipids in biological membranes (16). In addition, pyrene diffusion and excimer formation may be hampered by the inhomogeneity of the membrane. In order to verify that the difference in membrane dynamic characteristics originated from the phospholipids and not other, nonlipid, membrane constituents, we repeated the pyrene experiment with liposomes, which were reconstructed from purified phospholipids from cell membranes of opaque and transparent variants. Differences in lateral diffusion were most notable in liposomes, as pyrene excimerization rate constants were lower by 27 to 38% ($P \leq 0.05$) in the opaque variants than in the transparent variants, suggesting that the increased membrane microviscosity in the opaque variants was due, at least in part, to a different lipid composition.

An additional mode of motion, the rotational diffusion of the fatty acyl chains in the bilayer interior, was evaluated by fluorescence anisotropy, with DPH as a probe. It is a rodlike, highly hydrophobic molecule that intercalates into the membrane lipid core. DPH is oriented parallel to the axis of the lipid acyl chain, and its mode of motion is assumed to resemble the rotational diffusion of the lipid chains. Anisotropy changes are interpreted here in terms of microviscosity variation after verifying that the DPH lifetime did not change under the conditions studied. It is important to note that small changes (of about 10%) in fluorescence anisotropy may reflect pronounced changes (of about 25%) in membrane microviscosity (19). The results obtained with DPH show a 9 to 21% increase in the anisotropy values ($P \leq 0.001$) in the opaque variants compared with the trans-

parent variants, indicating an increase in membrane microviscosity of about 25%. These findings agree with the results obtained with pyrene, where lateral diffusion in the membrane of the opaque variant was lower than in the transparent variant, signifying higher microviscosity in bacteria with the opaque phenotype.

It was shown in *Escherichia coli* that changes in cell surface physical properties, such as phase transition temperature and membrane microviscosity, show a positive linear correlation with the proportion of unsaturated fatty acids in the bacterial lipids (14). In this study, the lipid acyl chain profile of four opaque-transparent *S. pneumoniae* strains shows that the two variants carry the same types of fatty acyl residues, mainly saturated and unsaturated straight C_{16} and C_{18} acids, as reported before for other strains of *S. pneumoniae* (24). However, the ratio of unsaturated to saturated fatty acids was increased in the transparent variants compared with the opaque variants. These results can explain the lower microviscosity observed in bacteria with the less saturated transparent phenotype. Preliminary data indicate that the enhancement of the desaturation index in the transparent variant is likely to result from an across the board increase in the desaturation level of the fatty acids, regardless of their lipid host. However, we are aware that changes in the ratio of membrane lipids may also have an effect on the properties of the different phenotypes. We are currently comparing the lipid distribution in the opaque variants with that in the transparent variants.

In general, introduction of double bonds into acyl chains can be achieved either anaerobically during fatty acid synthesis (13) or aerobically by modification of existing fatty acids through fatty acid desaturases (26). The cellular fatty acid composition is a result of a sum of complex phenomena maintaining optimal viability of the cell under various conditions. Therefore, it is difficult to understand the adjustment mechanisms linking fatty acid composition to various oxygen pressure or other stress factors.

The transition from benign pneumococcal colonization in the nasopharynx to invasive disease has been shown to be affected, both in vivo and in vitro, by the reversible phase variation in colony morphology from transparent to opaque. A molecular explanation for these divergent capabilities has begun to emerge from the understanding of the biochemical differences between the phenotypic variants. In this study we showed that the two variants differ in their membrane fluidity characteristics and fatty acid compositions. The function of the bacterial membrane response to environmental alterations, like oxygen availability, temperature, etc., can be rationalized on the basis of the advantages that it offers to the pneumococcus whose survival depends on variable environmental conditions. In general, tolerance to oxygen is known to involve enzyme-based detoxification and free radical scavenging mechanisms that have been described for many different organisms; these mechanisms are strongly induced by a mild oxidative burst (15). The decreased number of double bonds may confer an advantage on the opaque variants by decreasing their susceptibility to lipid peroxidation during an oxidative burst.

Further experiments will be carried out in our laboratory with genetically defined mutants that are essentially deficient in H_2O_2 production to show the effect of peroxide production on the biophysical characteristics and fatty acid composition of the membrane under various oxygen pressures. These experiments will provide more data on the adaptation processes endured by the pneumococcus under various environmental conditions.

REFERENCES

1. **Ackman, R. G.** 1969. Gas-liquid chromatography of fatty acids and esters. Methods Enzymol. **14:**329–381.
2. **Aguilar, P. S., A. M. Hernandez-Arriaga, L. E. Cybulski, A. C. Erazo, and D. de Mendoza.** 2001. Molecular basis of thermosensing: a two component signal transduction thermometer in *Bacillus subtilis*. EMBO J. **20:**1681–1691.
3. **Ames, G. F.** 1968. Lipids of *Salmonella typhimurium* and *Escherichia coli*: structure and metabolism. J. Bacteriol. **95:**833–843.
4. **Austrian, R.** 1976. The quellung reaction, a neglected microbiologic technique. Mt. Sinai J. Med. **43:**699–709.
5. **Binenbaum, Z., A. H. Parola, A. Zaritsky, and I. Fishov.** 1999. Transcription- and translation-dependent changes in membrane dynamics in bacteria: testing the transertion model for domain formation. Mol. Microbiol. **32:**1173–1182.
6. **Bligh, E. G., and W. J. Dyer.** 1959. A rapid method of total lipid extraction and purification. Can. J. Biochem. Physiol. **37:**911–917.
7. **Cohen, Z., H. A. Norman, and Y. M. Heimer.** 1993. Potential use of substituted pyridazinones for selecting polyunsaturated fatty acid overproducing cell lines of algae. Phytochemistry **32:**259–264.
8. **DeLong, E. F., and A. A. Yayanos.** 1985. Adaptation of the membrane lipids of a deep-sea bacterium to changes in hydrostatic pressure. Science **228:**1101–1103.
9. **Galla, H. J., and E. Sackman.** 1974. Lateral diffusion in the hydrophobic region of membranes: use of pyrene excimers as optical probes. Biochim. Biophys. Acta **339:**103–115.
10. **Guerzoni, M. E., R. Lanciotti, and S. Cocconcelli.** 2001. Alteration in cellular fatty acid composition as a response to salt, acid, oxidative and thermal stresses in *Lactobacillus helveticus*. Microbiology **147:**2255–2264.
11. **Kim, J. O., and J. N. Weiser.** 1998. Association of intrastrain variation in quantity of capsular polysaccharides and teichoic acid with the virulence of *Streptococcus pneumoniae*. J. Infect. Dis. **177:**368–377.
12. **Lanzetta, P. A., L. J. Alvarez, P. S. Reinach, and O. A. Candia.** 1979. An improved assay for nanomole amounts of inorganic phosphate. Anal. Biochem. **100:**95–97.
13. **Marrakchi, H., Y.-M. Zhang, and C. O. Rock.** 2002. Mechanistic diversity and regulation of type II fatty acid synthesis. Biochem. Soc. Trans. **30:**1050–1055.
14. **Mejia, R., M. C. Gomez-Eichelmann, and M. S. Fernandez.** 1999. Escherichia coli membrane fluidity as detected by excimerization of dipyrenylpropane: sensitivity to the bacterial fatty acid profile. Arch. Biochem. Biophys. **368:**156–160.
15. **Miller, R., and B. E. Britigan.** 1997. Role of oxidants in microbial pathophysiology. Clin. Microbiol. Rev. **10:**1–18.
16. **O'Leary, T. J.** 1987. Lateral diffusion of lipids in complex biological membranes. Proc. Natl. Acad. Sci. USA **84:**429–433.
17. **Porat, N., D. Gill, and A. H. Parola.** 1988. Adenosine deaminase in cell transformation: biophysical manifestation of membrane dynamics. J. Biol. Chem. **263:**14608–14611.
18. **Saluja, S. K., and J. N. Weiser.** 1995. The genetic basis of colony opacity in *Streptococcus pneumoniae*: evidence for the effect of box elements on the frequency of phenotypic variation. Mol. Microbiol. **16:**215–227.
19. **Shinitzky, M., and Y. Barenholz.** 1978. Fluidity parameters of lipid regions determined by fluorescence polarization. Biochim. Biophys. Acta **515:**367–394.
20. **Sinensky, M.** 1974. Homeoviscous adaptation—a homeostatic process that regulates the viscosity of membrane lipids in *Escherichia coli*. Proc. Natl. Acad. Sci. USA **71:**522–525.
21. **Soares, S., K. G. Kristinsson, J. M. Musser, and A. Tomasz.** 1993. Evidence for the introduction of a multiresistant clone of serotype 6B *Streptococcus pneumoniae* from Spain to Iceland in the late 1980s. J. Infect. Dis. **168:**158–163.
22. **Tedeschi, C., H. Mohwald, and S. Kirstein.** 2001. Polarity of layer-by-layer deposited polyelectrolyte films as determined by pyrene fluorescence. J. Am. Chem. Soc. **123:**954–996.
23. **Tomasz, A.** 2000. *Streptococcus pneumoniae*: functional anatomy, p. 9–21. *In*

A. Tomasz (ed.), *Streptococcus pneumoniae*: molecular biology and mechanisms of disease. Marry Ann Liebert, Inc., Publishers, Larchmont, N.Y.

24. **Trombe, M. C., M. A. Laneelle, and G. Laneelle.** 1979. Lipid composition of aminopterin-resistant and -sensitive strains of *Streptococcus pneumoniae*. Biochim. Biophys. Acta **574:**290–300.

25. **Vanounou, S., A. H. Parola, and I. Fishov.** 2003. Phosphatidylethanolamine and phosphatidylglycerol are segregated into different domains in bacterial membrane: a study with pyrene-labelled phospholipids. Mol. Microbiol. **49:** 1067–1079.

26. **Weber, M. H. W., W. Klein, L. Muller, U. M. NiesMarahiel.** 2001. Role of

Bacillus Subtilis fatty acid desaturase in membrane adaptation during cold shock. Mol. Microbiol. **39:**1321–1329.

27. **Weiser, J. N., R. Austrian, P. K. Sreenivasan, and H. R. Masure.** 1994. Phase variation in pneumococcal opacity: relationship between colonial morphology and nasopharyngeal colonization. Infect. Immun. **62:**2582–2589.

28. **Weiser, J. N.** 1998. Phase variation in colony opacity by *Streptococcus pneumoniae*. Microb. Drug Resist. **4:**129–135.

29. **Zaritsky, A., A. H. Parola, M. Ibdah, and H. Masalha.** 1985. Homeoviscous adaptation, growth rate, and morphogenesis in bacteria. Biophys. J. **48:**337–339.